ONLINE FIRST

This is a provisional PDF only. Copyedited and fully formatted version will be made available soon.

ISSN: 0015-5659

e-ISSN: 1644-3284

Therapeutic potential of stromal vascular fraction in early diabetic nephrotoxicity: a histomorphometric and immunohistochemical analysis in type 2 diabetes rat model

Authors: Amany Elsayed Hamoud, Hanaa Wanas, Ahmed Hamed Bayoumi, Doaa Mahmoud Shuaib, Maha Baligh Zickri, Mai Abdel Aziz Gouda, Ahmed Galal Motawie

DOI: 10.5603/fm.103545

Article type: Original article

Submitted: 2024-11-13

Accepted: 2025-01-09

Published online: 2025-01-16

Therapeutic potential of stromal vascular fraction in early diabetic nephrotoxicity: a histomorphometric and immunohistochemical analysis in type 2 diabetes rat model

Amany Elsayed Hamoud[1], Hanaa Wanas[2, 3], Ahmed Hamed Bayoumi[1, 4], Doaa Mahmoud Shuaib[1], Maha Baligh Zickri[5], Mai Abdel Aziz Gouda[6, 7], Ahmed Galal Motawie[1]

[1]Department of Anatomy, Kasr El-Aini Faculty of Medicine, Cairo University, Cairo, Egypt

[2]Department of Medical Pharmacology, Faculty of Medicine, Cairo University, Cairo, Egypt

[3]Department of Pharmacology and Toxicology, College of Pharmacy, Taibah University, Medina, Kingdom of Saudi Arabia

[4]Anatomy and Embryology Department, College of Medicine, Jouf University, Sakaka, Al-Jouf, Kingdom of Saudi Arabia

[5]Medical Histology and Cell Biology Department, Faculty of Medicine, Cairo University, Cairo, Egypt

[6]Biochemistry and Molecular Biology Faculty of Medicine, Cairo University, Cairo, Egypt

[7]Biochemistry and Molecular Biology, Badr University in Cairo, Badr, Egypt

Address for correspondence: Amany Elsayed Hamoud, Department of Anatomy, Kasr El-Aini Faculty of Medicine, Cairo University, Al Kasr Al Aini, Old Cairo, Cairo Governorate 4240310, Egypt; e-mail: dramanyhamoud@gmail.com

ABSTRACT

Background: Diabetic nephropathy (DN), a common complication of type 2 diabetes (T2D), significantly contributes to end-stage kidney disease (ESKD). Despite conventional treatments aimed at slowing disease progression, there is a pressing need for novel therapies. This study evaluates the potential therapeutic impact of adipose tissue derived stromal vascular fraction (SVF) on early diabetic nephrotoxicity in a rat model.

Materials and methods: Thirty-one male albino rats were divided into control and diabetic groups, with the latter further split into untreated (T2Da) and SVF-treated (T2Db) subgroups. Biochemical, histological, immunohistochemical, and morphometric analyses were conducted.
Results: We demonstrated that SVF treatment reduced oxidative stress, lowered serum creatinine, and improved renal architecture by mitigating fibrosis and cellular infiltration, suggesting enhanced tissue regeneration and reduced inflammation. SVF also facilitated cellular repair, indicated by increased endothelial cell proliferation and reduced glomerular damage.
Conclusions: This study underscores SVF's potential as a promising regenerative approach for managing early-stage DN, warranting further research to elucidate its mechanisms.
Keywords: SVF, diabetes, nephropathy, glomeruloscleosis

INTRODUCTION

Type 2 diabetes (T2D) mellitus has heterogeneous etiology. Hyperglycemia arising from impaired insulin action, production, or both, contributing to its pathogenesis. Diabetes mellitus is expected to affect 439 million people worldwide by 2030. Microvascular complications particularly diabetic nephropathy (DN), the most common complication of T2D, often resulting from prolonged disease duration. Since DN is a major risk factor for end-stage kidney disease (ESKD), early detection is essential to halting its progression [39]. Over the past few decades, there has been a strong correlation between the rise in obesity rates and the prevalence of T2D and the systemic immunological inflammation it causes. More than half of all instances of ESKD worldwide are currently caused by diabetic kidney disease (DKD), the most prevalent kind of chronic kidney disease [19].

To determine the risk of DKD, biochemical markers such as blood glucose levels, serum creatinine, and the number of neutrophils and lymphocytes are essential [42]. Comparing the neutrophil to lymphocyte ratio (NLR) to other inflammatory markers is of particular importance for detecting the risk of DKD in T2DM patients. Close monitoring of renal function should be carried out in situations of high NLR [26].

The standard treatment for individuals with or at risk of DKD has traditionally included renin-angiotensin system inhibitors, along with strict blood pressure and glucose control. Even while these treatments have been successful in postponing the deterioration in kidney function,

T2D induced ESKD is still prevalent, especially in middle-aged and obese individuals [45]. Accordingly, new therapy strategies are necessary to successfully stop the progression of DKD and enhance glomerular function and albuminuria outcomes [25].

A key goal in modern medicine is to restore normal function in acute or degenerative medical disorders by biologically enhancing of tissue regeneration and healing. In regenerative medicine, mesenchymal stem/stromal cells (MSCs), have garnered significant attention, particularly for their role in promoting repair. With encouraging outcomes in preclinical models, adipose tissue and its stromal vascular fraction (SVF) have recently been demonstrated to be a readily available source for MSCs and their products [34]. SVF has exerted therapeutic efficacy and safety throughout different clinical studies by improvement of tissue regeneration [18]. Additionally, SVF-gel formed of granular fat, enriched with adipose stem cells is recently applied in treatment of various skin lesions [26].

This study used serological, biochemical, histological, histochemical, immunohistochemical, and morphometric investigations to explore the potential role of stromal vascular fraction therapy in treating early nephrotoxicity induced by T2D in adult male albino rats.

MATERIALS AND METHODS

Materials

Drugs

Sigma Company (St. Louis, MO, USA) provided streptozotocin in a 1 gram (g) vial in powdered form. A digital scale was used to weigh the necessary dosage, which was then dissolved in citrate buffer.

Adipose tissue collection, Processing and Isolation of SVF

Approximately 20 g of adipose tissue was harvested from the abdominal fat of each rat under aseptic conditions following a small skin incision in the lower abdomen under general anesthesia (phenobarbitone sodium, 60 mg/kg). The tissue was treated using under a sterile laminar airflow. The fat was finely minced, then rinsed three times with phosphate-buffered saline (PBS) before an equal volume of 0.1% collagenase type I was added. In a rotating incubator, the mixture was incubated for an hour at 37°C while being constantly stirred. After digestion, the collagenase was neutralized by adding an equivalent volume of Dulbecco's

Modified Eagle's Medium (DMEM) containing 10% fetal bovine serum. The collagenase was then separated from the SVF by centrifuging it for 10 minutes at 800 *g*. [20]. To get rid of any remaining collagenase, the SVF was then rinsed three times with PBS. Following the final centrifugation cycle, trypan blue staining and hemocytometer counting were performed.

In vitro *SVF expansion*

The cell pellet was suspended in media at a 10:1 media-to-cell volume ratio. With a final media volume of 10 ml, cells were planted in a culture flask at a density of 30–50% confluence. The flasks were kept in an atmosphere with 5% CO_2 at 37°C. The adherent cells were able to achieve 80–90% confluence after the media was changed after 24 hours to exclude non-adherent cells. After that, 1×10^6 adipose-derived mesenchymal stem cells (AD-MSCs) were injected into the culture after being resuspended in PBS [36].

Immunophenotyping of AD-MSCs (flow cytometry)

After the second passage, stem cells were washed and incubated for 5–10 minutes with a 10% trypsin EDTA solution. The cell pellet was then treated with a primary antibody against the cell surface marker CD44 in 1% bovine serum albumin and incubated for one hour. A secondary antibody was added for 30 minutes prior to analysis using a fluorescence-activated cell sorting (FACS) analyzer [31].

Animals and experimental design

Thirty-one male albino rats, each weighing 100 grams and aged four weeks, were used in this investigation. The animals were housed at the Animal House of the Faculty of Medicine, Kasr Al-Ainy, Cairo University, under standard conditions: temperature of 25 ± 2°C, humidity of 60 ± 10%, and a 12-hour light/dark cycle (lights on at 6:00 am). They were individually housed in wire cages with free access to food and water. The experiment adhered to the Cairo University Institutional Animal Care and Use Committee (IACUC) guidelines (CU-III-F-23-24) and followed ARRIVE guidelines [35].

The rats were randomly assigned to the following groups:

1. **Donor group:** five rats were used for adipose tissue collection, SVF isolation, and flow cytometry for immunophenotyping.

2. **Control group (C):** six rats were maintained on a normal chow diet (ND) for 10 weeks and 3 days, with an average final weight of 150–180 grams. They were divided into two subgroups:

- **(Ca):** three rats received a single intraperitoneal (IP) injection of 0.5 ml citrate buffer [the solvent for streptozotocin (STZ)] 4 weeks after the experiment's start.
- **(Cb):** three rats received 0.5 mL citrate buffer as in subgroup Ca. After an additional 4 weeks and 3 days, they were administered 1 mL phosphate-buffered saline (PBS) (the SVF suspension) via IP injection once.

3. **Type 2 diabetic (T2D) group:** twenty rats were fed a high-fat diet (HFD) consisting of 60% fat, 20% carbohydrates, and 20% protein [28] for 4 weeks, reaching a body weight of 250–280 grams to induce insulin resistance. Following an overnight fast, each rat received a single low-dose intraperitoneal injection of STZ (40 mg/kg, dissolved in 0.5 mL citrate buffer at pH 4.2–4.5) [21]. Blood glucose levels were measured after three days, and rats with levels exceeding 200 mg/dL were diagnosed with T2D [22]. Four weeks post-diabetes confirmation, 6 rats were sacrificed for histological confirmation of early nephropathy [12]. The remaining diabetic rats were further equally subdivided into the following subgroups:

- **T2Da (spontaneous recovery subgroup):** seven rats were observed for an additional 2 weeks without intervention.
- **T2Db (SVF treated subgroup):** Seven rats each received an IP injection of adipose-derived (AD) SVF containing 1×10^6 Ferridex-labeled cells suspended in 1 mL PBS, with a follow-up period of 2 weeks [14].

All animals were sacrificed after 10 weeks and 3 days from the start of the experiment.

Animal sacrifice and specimen collection

Control, diabetic, and treated rats were anesthetized with phenobarbitone sodium (60 mg/kg, IP) and euthanized by cervical dislocation [15, 44]. A midline incision was performed to expose and excise the kidneys, with further processing and analyses.

Serological evaluation

Prior to sacrifice, blood samples were drawn from the tail vein for blood glucose and creatinine levels estimation after 10 weeks and 3 days from the start of the experiment.

Biochemical assessment

Left kidney specimens were homogenized in 1 mL normal saline and stored at –20°C. The homogenates were centrifuged at 1000 *g* for 15 minutes, and the supernatants were stored at –20°C in Eppendorf tubes [37]. Using colorimetric assay kits, tissue homogenates were analyzed for malondialdehyde (MDA), oxidative stress marker [4], catalase (CAT), antioxidant enzyme [46]. And hydroxyproline, collagen content marker [48], were determined using biodiagnostic colorimetric assay kits in tissue homogenates (Biodiagnostic, Cairo, Egypt).

Histological study

Right kidney specimens were preserved in 10% formal saline for 48 hours, and 5 μm sections were prepared from paraffin blocks for staining. Haematoxylin and eosin (H&E) was used for general tissue morphology [24]. Masson's Trichrome (MT) was used for collagen fiber detection [5].

Histochemical study

Perls' Prussian Blue (Pb) stain was used to detect the homing of Feridex-labeled AD-MSCs within the kidney samples. AD-MSCs were obtained from *in vitro* SVF expansion [11].

Immunohistochemical study [38]

Proliferating Cell Nuclear Antigen (PCNA) was used as a marker for cell regeneration. PCNA immunostaining employed a prediluted primary mouse monoclonal antibody (Clone PC10, Lab Vision Corporation, Fremont, CA, USA) with 0.1 mL added for 60 minutes. Human skin served as a positive control, and a negative control was prepared by omitting the primary antibody [10].

Morphometric study

Five non-overlapping fields were analyzed using Leica Qwin 500 LTD software (Cambridge, UK). Quantitative assessments included glomerular area, the number of PCNA-positive

endothelial and mesangial nuclei, and PCNA-positive interstitial nuclei area. Additionally, the collagen fiber area percentage in the cortex and medulla was calculated in binary mode.

Statistical Study [7]

Analysis of variance (ANOVA) was used to compare the quantitative data, which was summarised as means and standard deviations. To determine which group pairs were responsible for the significant difference, the Bonferroni *post-hoc* test was employed after every significant (sig) ANOVA. Statistical significance was defined as p-values less than 0.05. The statistical package of the social sciences (SPSS) version 18.0 for Windows (IBM Corporation, Armonk, NY, USA) was used to do the calculations.

RESULTS

Immunophenotyping of AD-MSCs

Adipose derived MSCs appeared mostly spindle (Fig. 1A), with immunophenotyping indicating a 93.9% positive expression rate (Fig. 1B).

Serological assessment

The mean values of blood glucose were (89.51 ± 2.53 mg/dL), (310.09 ± 9.11 mg/dL) and (100.4 ± 7.54 mg/dL) in groups C, subgroups T2Da and T2Db respectively. While, the mean values of serum creatinine were (0.39 ± 0.03 mg/dL), (1.61 ± 0.15 mg/dL) and (0.54 ± 0.06 mg/dL) respectively. Notably, the **Spontaneous recovery subgroup** (T2Da subgroup) exhibited a significant increase in blood glucose and serum creatinine levels compared to both the **control group** (C group) and the **SVF treated subgroup** (T2Db subgroup), as illustrated in (Figs. 1C and 1D).

Biochemical assessment

Biochemical assessments of oxidative stress markers revealed that the malondialdehyde (MDA) and catalase (CAT) levels were (4.72 ± 0.04 μmol/g) and (12.94±0.55 U/g) in **C group**, (14.93 ± 2.54 μmol/g) and (4.85 ± 1.01 U/g) in **T2Da subgroup**, (5.02 ± 0.24 μmol/g) and (11.21 ± 1.15 U/g) in **T2Db subgroup**. The **T2Da subgroup** showed a significant increase in MDA and a decrease in CAT compared to both the **C group** and **T2Db subgroup**, as seen in (Fig. 1E).

Histological results

In H&E stained sections, Figure 2 showed in C group, the renal cortex exhibiting distal tubules with wide lumen, proximal tubules with strong acidophilic cytoplasm, and Malpighian corpuscles with patent Bowman's space. The collecting tubules in the medulla showed wide lumen and pale cytoplasm (Figs. 2 A, B). The **T2Da subgroup** showed dense cellular infiltration among the cortical tubules, a number of distended glomeruli with obliterated Bowman's space, shrunken glomeruli, vacuolations in the cortical tubules and congestion among the collecting tubules (Figs. 2C–F).

Figure 3 showed in **T2Da subgroup** multiple fibroblasts detected around congested peritubular capillaries and multiple vacuolations detected among the collecting tubules (Figs. 3A, B). In **T2Db subgroup,** minimal cellular infiltrate was found among the cortical tubules and few shrunken glomeruli were evident in few fields. Minimal congestion and few vacuolations were observed among apparently normal collecting tubules (Figs 3C–F).

In **Trichrome stained renal sections**, Figure 4 revealed in **C group**, fine collagen fibers between cortical and collecting tubules (Figs. 4A, B). In **T2Da subgroup**, dense collagen bundles were seen in the cortical and reticular in collecting tubules (Figs. 4C, D). In **T2Db subgroup**, a few regions between the cortical or collecting tubules, occasionally displayed dense or reticular collagen bundles (Figs. 4E, F).

Histochemical results

In **Pb stained sections**, Figure 4 demonstrated in **T2Db subgroup** numerous positively stained spindle cells dispersed throughout the renal glomeruli, cortical and collecting tubules (Figs. 4G, H).

Immunohistochemical results

In **PCNA immunostained sections,** Figure 5 recruited **in C group** few +ve nuclei of the lining of proximal and distal tubules, in addition to some +ve flat nuclei and occasional +ve round nuclei among the glomeruli. Few +ve nuclei of the lining of collecting tubules were seen (Figs. 5A–C). In **T2Da subgroup,** multiple +ve round nuclei and few +ve flat nuclei were observed among distended glomeruli**,** besides some +ve round nuclei and few +ve flat nuclei were seen

among shrunken glomeruli. In addition**,** multiple +ve nuclei were detected among the cortical and collecting tubules, that appeared as flat interstitial nuclei between the cortical and collecting tubules by close observation (Figs. 5D–I). In **T2Db subgroup,** multiple +ve flat nuclei and few +ve round nuclei were seen among the glomeruli. In addition, some +ve nuclei were evident among the tubules at the corticomedullary junction, identified as +ve flat interstitial nuclei between the tubules by close observation (Figs. 5J–L).

Morphometric results

Comparing the T2Da subgroup to the C group and T2Db subgroup, the morphometric analysis showed a substantial increase in mean glomerular area and mean collagen area% in both the cortex and the medulla. Furthermore, T2Da subgroup had significantly lower mean count of PCNA +ve endothelial nuclei. Whereas, T2Da subgroup had significantly higher mean count of PCNA +ve mesangial nuclei and mean area of PCNA +ve interstitial nuclei (Tab. 1).

DISCUSSION

Over half of end-stage kidney disease is caused by diabetic kidney disease (DKD). Due to the higher frequency of T2DM linked to obesity, even in its early stages, DKD has become the most common chronic kidney disease worldwide [26]. The current study sought to assess the potential effectiveness of the stromal-vascular fraction and create an experimental model of T2D-induced early nephrotoxicity using serological, biochemical, histological, histochemical, immunohistochemical and morphometric studies.

The untreated T2Da subgroup's serum glucose and creatinine levels were significantly higher than those of the control (C) group and the SVF-treated T2Db subgroup. This is consistent with the complicated pathophysiology of type 2 diabetes, where hyperglycemia need careful control to avoid complications [8]. The cellular components of SVF, a developing treatment for type 2 diabetes, have been shown to activate angiogenesis, regenerate pancreatic islet beta cells, lower inflammation, and reduce oxidative stress [23]. In both human and animal models, elevated creatinine levels are known to be a sign of early renal impairment [2, 3]. SVF therapy has been demonstrated to lower serum creatinine levels [6], which is in line with the results in our T2Db subgroup.

In the present study, elevated MDA and decreased CAT levels in the T2Da subgroup indicated a significant oxidative imbalance. Oxidative stress, which is associated with type 2 diabetes, is connected to insulin resistance, ß-cell dysfunction, metabolic dysregulation, and diabetic consequences such as nephrotoxicity [32]. As shown in the T2Da subgroup, oxidative stress is commonly characterized by elevated tissue MDA and decreased CAT levels. The potential of SVF to restore the oxidant-antioxidant balance is suggested by the improvement in oxidative markers observed in the T2Db subgroup that received SVF treatment.

Histological examination showed clear variations in kidney shape between the groups. The appearance of fibroblasts surrounding crowded peritubular capillaries, congestion in collecting tubules, and extensive cellular infiltration among cortical tubules all suggested inflammation in the untreated T2Da subgroup. This is consistent with research on inflammatory cell infiltration in diabetic nephropathy [41]. Furthermore, poor renal function has been associated with venous congestion, a characteristic of congestion-related nephropathy [9].

Further observations in the T2Da subgroup included multiple distended and shrunken glomeruli and vacuolations among cortical and collecting tubules, suggesting progressive inflammatory changes leading to glomerulosclerosis and glomerular atrophy. This was confirmed morphometrically and indicates tubular degenerative changes Fareed et al. [13] and Ma et al. [30]. reported that high levels of reactive oxygen species (ROS) in diabetic nephropathy activate pathways that damage the antioxidant defense system, disrupt vascular permeability, and induce glomerular proliferation before atrophy. Glomerular shrinkage and tubulointerstitial injury, as seen in our study, are also well-documented features of diabetic nephropathy [1, 29].

According to our results, there was less cellular infiltration, less glomerular shrinkage, less collecting tubule congestion, and less tubular epithelial cell vacuolation in the SVF-treated T2Db subgroup. SVF, enriched with mesenchymal stem cells (MSCs), supports tissue repair, regeneration, and immunomodulation, according to Ossendorff et al. [34] and Vargel et al. [40]. Additionally, Goncharov et al. [18] showed that SVF's immunomodulatory and anti-inflammatory properties support tissue repair and regeneration. Furthermore, trichrome-stained sections showed that the T2Db subgroup had fewer collagen deposits than the untreated group, suggesting that the fibrotic alterations had subsided. According to Xue et al. [41], renal fibrosis is a major pathology in T2DM-induced nephropathy. The extracellular matrix in SVF, which

promotes cell survival and differentiation, and the regenerative plasticity of MSCs may be responsible for the reduction in fibrosis observed with SVF treatment [27, 43].

Histochemical analysis using Prussian blue staining showded multiple positively stained spindle cells in the renal cortex and medulla, suggesting mesenchymal stem cell homing in the SVF-treated group. Prussian blue staining is known to identify iron labeling in these cells, providing evidence of cellular retention and localization in the kidney [16].

In the T2Da subgroup, PCNA immunostaining revealed a large number of positive nuclei, especially in the interstitial spaces and reduced glomeruli, indicating increased cellular proliferation. A notable reduction in PCNA-positive endothelial nuclei and a rise in PCNA-positive mesangial and interstitial nuclei supported this, indicating cellular proliferation linked to diabetic nephropathy's damage and healing processes. According to Oliva-Damaso et al. [33] mesangial proliferation rises in diabetic nephropathy while endothelium proliferation falls. The SVF-treated T2Db subgroup, on the other hand, showed elevated endothelium PCNA positive, suggesting restorative activity as opposed to unchecked proliferation. The regenerative properties of SVF components, such as adipose-derived stem cells, which support angiogenesis, tissue remodeling, and immunomodulation, are consistent with this finding [10, 47].

This study concludes by highlighting SVF's therapeutic potential in reducing the early nephrotoxic consequences of type 2 diabetes. In kidney tissues, SVF therapy enhanced oxidative stress indicators, decreased inflammation, eased fibrosis, and encouraged cellular regeneration. Although more research is necessary to fully understand SVF's exact mechanisms of action in renal repair, our results point to SVF as a potentially effective treatment option for diabetic nephropathy.

ARTICLE INFORMATION AND DECLARATIONS

Data availability statement

All supporting data for this work are available on request from the corresponding author.

Ethics statement

The experiment adhered to the Cairo University Institutional Animal Care and Use Committee (IACUC) guidelines (CU-III-F-23-24) and followed ARRIVE guidelines.

Author contributions

Hamoud A. and Zickri M. conceived and designed the paper work. Zickri M., Hanaa Wanas and Hamoud A. analyzed and interpreted the results of experiments. Hamoud A. and Shauaib D. prepared the figures. Galal A. and AbdelAziz M. performed the biochemical analysis. Hamoud A., Hanaa Wanas and Zickri M. drafted the manuscript. Hamed A performed the critical editing of the manuscript.

Funding

The authors did not receive any funding.

Acknowledgments

The authors would like to extend their appreciation to Dr. Laila Rashed for her supervision and support.

Conflict of interest

The authors declare that there is no conflict interest

REFERENCES

1. Ahmed A, Salama E, Shehata H, et al. The role of Ischemia modified albumin in detecting diabetic nephropathy. SVU Int J Med Sci. 2023; 6(1): 359–367, doi: 10.21608/svuijm.2022.165289.1419.
2. Al-Qabbaa SM, Qaboli SI, Alshammari TK, et al. Sitagliptin mitigates diabetic nephropathy in a rat model of streptozotocin-induced type 2 diabetes: possible role of PTP1B/JAK-STAT pathway. Int J Mol Sci. 2023; 24(7), doi: 10.3390/ijms24076532, indexed in Pubmed: 37047505.
3. Asmamaw T, Genet S, Menon M, et al. Early detection of renal impairment among patients with type 2 diabetes mellitus through evaluation of serum cystatin c in

comparison with serum creatinine levels: a cross-sectional study. Diabetes Metab Syndr Obes. 2020; 13: 4727–4735, doi: 10.2147/DMSO.S279949, indexed in Pubmed: 33299336.

4. Atia T, Iqbal MZ, Fathy Ahmed H, et al. Vitamin d supplementation could enhance the effectiveness of glibenclamide in treating diabetes and preventing diabetic nephropathy: a biochemical, histological and immunohistochemical study. J Evid Based Integr Med. 2022; 27: 2515690X221116403, doi: 10.1177/2515690X221116403, indexed in Pubmed: 35942573.
5. Bancroft JD, Gamble M. Connective tissue stains. In: Bancroft JD, Gamble M. ed. Theory and practice of histological techniques, 6th ed. Elsevier Health Science, Edinburgh 2008.
6. Carstens MH, García N, Mandayam S, et al. Safety of stromal vascular fraction cell therapy for chronic kidney disease of unknown cause (mesoamerican nephropathy). Stem Cells Transl Med. 2023; 12(1): 7–16, doi: 10.1093/stcltm/szac080, indexed in Pubmed: 36545894.
7. Dalmaijer ES, Nord CL, Astle DE. Statistical power for cluster analysis. BMC Bioinformatics. 2022; 23(1): 205, doi: 10.1186/s12859-022-04675-1, indexed in Pubmed: 35641905.
8. Davies MJ, Aroda VR, Collins BS, et al. Management of hyperglycemia in type 2 diabetes, 2022. A consensus report by the american diabetes association (ADA) and the european association for the study of diabetes (EASD). Diabetes Care. 2022; 45(11): 2753–2786, doi: 10.2337/dci22-0034, indexed in Pubmed: 36148880.
9. D'Marco L. Congestive nephropathy. Int J Environ Res Public Health. 2022; 19(5): 2499, doi: 10.3390/ijerph19052499, indexed in Pubmed: 35270191.
10. Dong Xi, Lu S, Tian Yu, et al. Bavachinin protects the liver in NAFLD by promoting regeneration via targeting PCNA. J Adv Res. 2024; 55: 131–144, doi: 10.1016/j.jare.2023.02.007, indexed in Pubmed: 36801384.

11. Doroudian M, O'Neill A, O'Reilly C, et al. Aerosolized drug-loaded nanoparticles targeting migration inhibitory factors inhibit Pseudomonas aeruginosa-induced inflammation and biofilm formation. Nanomedicine (Lond). 2020; 15(30): 2933–2953, doi: 10.2217/nnm-2020-0344, indexed in Pubmed: 33241979.

12. El-Kady MM, Naggar RA, Guimei M, et al. Early renoprotective effect of ruxolitinib in a rat model of diabetic nephropathy. Pharmaceuticals (Basel). 2021; 14(7), doi: 10.3390/ph14070608, indexed in Pubmed: 34202668.

13. Fareed SA, Yousef EM, Abd El-Moneam SM. Assessment of effects of rosemary essential oil on the kidney pathology of diabetic adult male albino rats. Cureus. 2023; 15(3): e35736, doi: 10.7759/cureus.35736, indexed in Pubmed: 37016650.

14. Farid MF, Abouelela YS, Yasin NAE, et al. Laser-activated autologous adipose tissue-derived stromal vascular fraction restores spinal cord architecture and function in multiple sclerosis cat model. Stem Cell Res Ther. 2023; 14(1): 6, doi: 10.1186/s13287-022-03222-2, indexed in Pubmed: 36627662.

15. García-Pedraza JÁ, García-Domingo M, Gómez-Roso M, et al. Hypertension exhibits 5-HT receptor as a modulator of sympathetic neurotransmission in the rat mesenteric vasculature. Hypertens Res. 2019; 42(5): 618–627, doi: 10.1038/s41440-019-0217-7, indexed in Pubmed: 30696976.

16. Geng W, Zhang Z, Yang Z, et al. Non-aqueous synthesis of high-quality Prussian blue analogues for Na-ion batteries. Chem Commun (Camb). 2022; 58(28): 4472–4475, doi: 10.1039/d2cc00699e, indexed in Pubmed: 35297912.

17. Goncharov EN, Koval OA, Igorevich EI, et al. Analyzing the clinical potential of stromal vascular fraction: a comprehensive literature review. Medicina (Kaunas). 2024; 60(2), doi: 10.3390/medicina60020221, indexed in Pubmed: 38399509.

18. Goncharov EN, Koval OA, Nikolaevich Bezuglov E, et al. Comparative analysis of stromal vascular fraction and alternative mechanisms in bone fracture stimulation to bridge the gap between nature and technological advancement: a systematic review. Biomedicines. 2024; 12(2), doi: 10.3390/biomedicines12020342, indexed in Pubmed: 38397944.

19. Guo W, Song Y, Sun Y, et al. Systemic immune-inflammation index is associated with diabetic kidney disease in Type 2 diabetes mellitus patients: evidence from NHANES 2011-2018. Front Endocrinol (Lausanne). 2022; 13: 1071465, doi: 10.3389/fendo.2022.1071465, indexed in Pubmed: 36561561.

20. Hayashi S, Yagi R, Taniguchi S, et al. A novel method for processing adipose-derived stromal stem cells using a closed cell washing concentration device with a hollow fiber membrane module. Biomed Microdevices. 2021; 23(1): 3, doi: 10.1007/s10544-020-00541-0, indexed in Pubmed: 33404966.

21. Huang Q, Tian H, Tian L, et al. Inhibiting Rev-erbα-mediated ferroptosis alleviates susceptibility to myocardial ischemia-reperfusion injury in type 2 diabetes. Free Radic Biol Med. 2023; 209(Pt 1): 135–150, doi: 10.1016/j.freeradbiomed.2023.09.034, indexed in Pubmed: 37805047.

22. Ighodaro OM, Adeosun AM, Ujomu TS, et al. Combination therapy of Allium cepa L. and Cucumis sativa L. extracts in streptozotocin-induced diabetic rat model. Futur J Pharm Sci. 2021; 7(1): 227–234, doi: 10.1186/s43094-021-00371-8.

23. Karina K, Krisandi G, Rosadi I, et al. Stromal vascular fraction and autologous activated platelet-rich plasma combination in treatment of type 2 diabetes: a single center retrospective study. Clin Diabetol. 2023; 12(4): 247–252, doi: 10.5603/dk.a2023.0027.

24. Kiernan JA. Histological and histochemical methods: Theory and practice. 5th edition. Arnold, London 2015: 132–212.

25. Kim DL, Lee SE, Kim NH. Renal protection of mineralocorticoid receptor antagonist, finerenone, in diabetic kidney disease. Endocrinol Metab (Seoul). 2023; 38(1): 43–55, doi: 10.3803/EnM.2022.1629, indexed in Pubmed: 36891650.

26. Li M, Tian Y, Cheng R, et al. Clinical efficacy of stromal vascular fraction gel in the treatment of mature striae distensae. Skin Res Technol. 2024; 30(1): e13551, doi: 10.1111/srt.13551, indexed in Pubmed: 38221781.

27. Li X, Wang L, Liu M, et al. Association between neutrophil-to-lymphocyte ratio and diabetic kidney disease in type 2 diabetes mellitus patients: a cross-sectional study. Front

Endocrinol (Lausanne). 2023; 14: 1285509, doi: 10.3389/fendo.2023.1285509, indexed in Pubmed: 38239986.

28. Liao Z, Kong Y, Zeng L, et al. Effects of high-fat diet on thyroid autoimmunity in the female rat. BMC Endocr Disord. 2022; 22(1): 179, doi: 10.1186/s12902-022-01093-5, indexed in Pubmed: 35840950.

29. Luo WM, Su JY, Xu T, et al. Prevalence of diabetic retinopathy and use of common oral hypoglycemic agents increase the risk of diabetic nephropathy — a cross-sectional study in patients with type 2 diabetes. Int J Environ Res Public Health. 2023; 20(5), doi: 10.3390/ijerph20054623, indexed in Pubmed: 36901633.

30. Ma X, Ma J, Leng T, et al. Advances in oxidative stress in pathogenesis of diabetic kidney disease and efficacy of TCM intervention. Ren Fail. 2023; 45(1): 2146512, doi: 10.1080/0886022X.2022.2146512, indexed in Pubmed: 36762989.

31. Meligy FY, Abo Elgheed AT, Alghareeb SM. Therapeutic effect of adipose-derived mesenchymal stem cells on Cisplatin induced testicular damage in adult male albino rat. Ultrastruct Pathol. 2019; 43(1): 28–55, doi: 10.1080/01913123.2019.1572256, indexed in Pubmed: 30741078.

32. Najafi A, Pourfarzam M, Zadhoush F. Oxidant/antioxidant status in type-2 diabetes mellitus patients with metabolic syndrome. J Res Med Sci. 2021; 26: 6, doi: 10.4103/jrms.JRMS_249_20, indexed in Pubmed: 34084185.

33. Oliva-Damaso N, Mora-Gutiérrez JM, Bomback AS. Glomerular diseases in diabetic patients: implications for diagnosis and management. J Clin Med. 2021; 10(9), doi: 10.3390/jcm10091855, indexed in Pubmed: 33923227.

34. Ossendorff R, Menon A, Schildberg FA, et al. A worldwide analysis of adipose-derived stem cells and stromal vascular fraction in orthopedics: current evidence and applications. J Clin Med. 2023; 12(14), doi: 10.3390/jcm12144719, indexed in Pubmed: 37510834.

35. Sert NP, Hurst V, Ahluwalia A, et al. The ARRIVE guidelines 2.0: Updated guidelines for reporting animal research. PLOS Biol. 2020; 18(7): e3000410, doi: 10.1371/journal.pbio.3000410, indexed in Pubmed: 32663219.

36. Sekiya I, Larson BL, Smith JR, et al. Expansion of human adult stem cells from bone marrow stroma: conditions that maximize the yields of early progenitors and evaluate their quality. Stem Cells. 2002; 20(6): 530–541, doi: 10.1634/stemcells.20-6-530, indexed in Pubmed: 12456961.

37. Shi Q, Wang J, Cheng Y, et al. Palbinone alleviates diabetic retinopathy in STZ-induced rats by inhibiting NLRP3 inflammatory activity. J Biochem Mol Toxicol. 2020; 34(7): e22489, doi: 10.1002/jbt.22489, indexed in Pubmed: 32202043.

38. Suvarna SK, Layton C, Bancroft JD. Immunohistochemical and immunofluorescent techniques. In: Suvarna SK, Layton C, Bancroft JD. ed. Bancroft's Theory and practice of histological techniques. 8th ed. Elsevier, Beijing 2019: 337–394.

39. Thipsawat S. Early detection of diabetic nephropathy in patient with type 2 diabetes mellitus: A review of the literature. Diab Vasc Dis Res. 2021; 18(6): 14791641211058856, doi: 10.1177/14791641211058856, indexed in Pubmed: 34791910.

40. Vargel İ, Tuncel A, Baysal N, et al. Autologous adipose-derived tissue stromal vascular fraction (AD-tSVF) for knee osteoarthritis. Int J Mol Sci. 2022; 23(21), doi: 10.3390/ijms232113517, indexed in Pubmed: 36362308.

41. Xue R, Xiao H, Kumar V, et al. The molecular mechanism of renal tubulointerstitial inflammation promoting diabetic nephropathy. Int J Nephrol Renovasc Dis. 2023; 16: 241–252, doi: 10.2147/IJNRD.S436791, indexed in Pubmed: 38075191.

42. Yan P, Yang Y, Zhang X, et al. Association of systemic immune-inflammation index with diabetic kidney disease in patients with type 2 diabetes: a cross-sectional study in Chinese population. Front Endocrinol (Lausanne). 2023; 14: 1307692, doi: 10.3389/fendo.2023.1307692, indexed in Pubmed: 38239983.

43. Yang J, Wang X, Zeng X, et al. One-step stromal vascular fraction therapy in osteoarthritis with tropoelastin-enhanced autologous stromal vascular fraction gel. Front Bioeng Biotechnol. 2024; 12: 1359212, doi: 10.3389/fbioe.2024.1359212, indexed in Pubmed: 38410163.

44. Yaşar M, Çakmak H, Dündar S, et al. The role of microRNAs in corneal neovascularization and its relation to VEGF. Cutan Ocul Toxicol. 2020; 39(4): 341–347, doi: 10.1080/15569527.2020.1813749, indexed in Pubmed: 32854552.

45. Zanchi A, Jehle AW, Lamine F, et al. Diabetic kidney disease in type 2 diabetes: a consensus statement from the Swiss Societies of Diabetes and Nephrology. Swiss Med Wkly. 2023; 153: 40004, doi: 10.57187/smw.2023.40004, indexed in Pubmed: 36652726.

46. Zhang L, Chu W, Zheng L, et al. Zinc oxide nanoparticles from Cyperus rotundus attenuates diabetic retinopathy by inhibiting NLRP3 inflammasome activation in STZ-induced diabetic rats. J Biochem Mol Toxicol. 2020; 34(12): e22583, doi: 10.1002/jbt.22583, indexed in Pubmed: 32692483.

47. Zhao X, Guo J, Zhang F, et al. Therapeutic application of adipose-derived stromal vascular fraction in diabetic foot. Stem Cell Res Ther. 2020; 11(1): 394, doi: 10.1186/s13287-020-01825-1, indexed in Pubmed: 32928305.

48. Zohny MH, Cavalu S, Youssef ME, et al. Coomassie brilliant blue G-250 dye attenuates bleomycin-induced lung fibrosis by regulating the NF-κB and NLRP3 crosstalk: a novel approach for filling an unmet medical need. Biomed Pharmacother. 2022; 148: 112723, doi: 10.1016/j.biopha.2022.112723, indexed in Pubmed: 35202914.

Table 1. Summary of morphometric results.

Group and subgroups	**Mean GA**	**Mean C area% in Cx**	**Mean C area% in M**	**Mean count of PCNA +ve eN**	**Mean count of PCNA +ve mN**	**Mean area of PCNA +ve iN**
C group	4004.25 ± 20.99	3.29 ± 0.15	2.95 ± 0.23	5.1 ± 0.02	1.4 ± 0.25	0
T2Da subgroup	6255.43 ± 45.83*	18.93 ± 2.09*	9.98 ± 2.25*	2.4 ± 0.21*	4.5 ± 0.46*	4857.85 ± 31.98
T2Db	3992.42 ±	3.98 ± 0.31	3.26 ± 0.33	6.9 ± 0.12	1.9 ± 0.21	1599.51 ±

subgroup	28.69					17.85

*Significant ($p \leq 0.05$) versus C group and T2Db subgroup. PCNA — proliferating cell nuclear antigen.

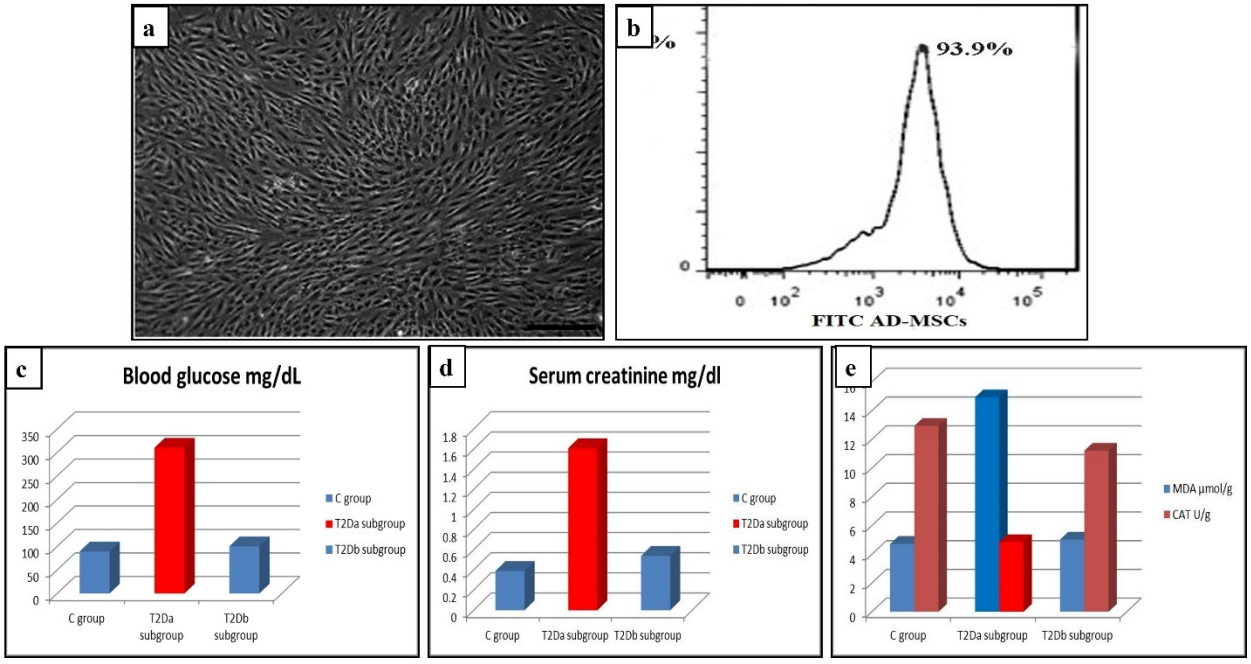

Figure 1A. AD-MSCs mostly spindle (inverted microscope, ×100); **B.** Immuno-phenotyping denoting 93.9%; **C.** Histogram of mean values of blood glucose in mg/dL; **D.** Histogram of mean values of serum creatinine in mg/dL); **E.** Histogram of mean values of MDA in μmol/g and CAT in U/g. AD-MSCs — adipose-derived mesenchymal stem cells; CAT — catalase; MDA — malondialdehyde.

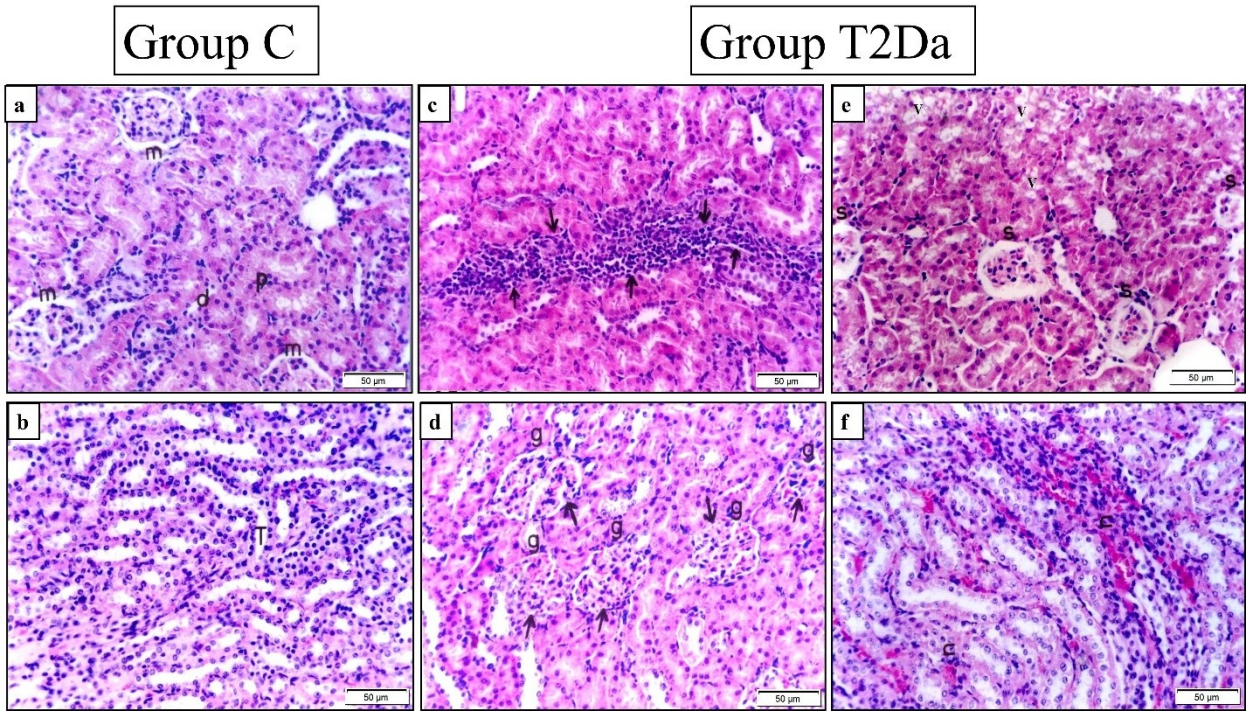

Figure 2. Haematoxylin and eosin, (×200) stained kidney sections revealed: **A.** Renal cortex exhibiting Malpighian corpuscles (m), proximal tubules (p) and distal tubules (d); **B.** Renal medulla exhibiting collecting tubules (T) **in C group; C**. Dense cellular infiltrate among the cortical tubules; **D.** Multiple distended glomeruli (g) and obliterated BS (arrows); **E.** Multiple shrunken (s) glomeruli and multiple vacuolations (v) among the cortical tubules; **F.** Obvious congestion (c) among the collecting tubules **in subgroup T2Da**.

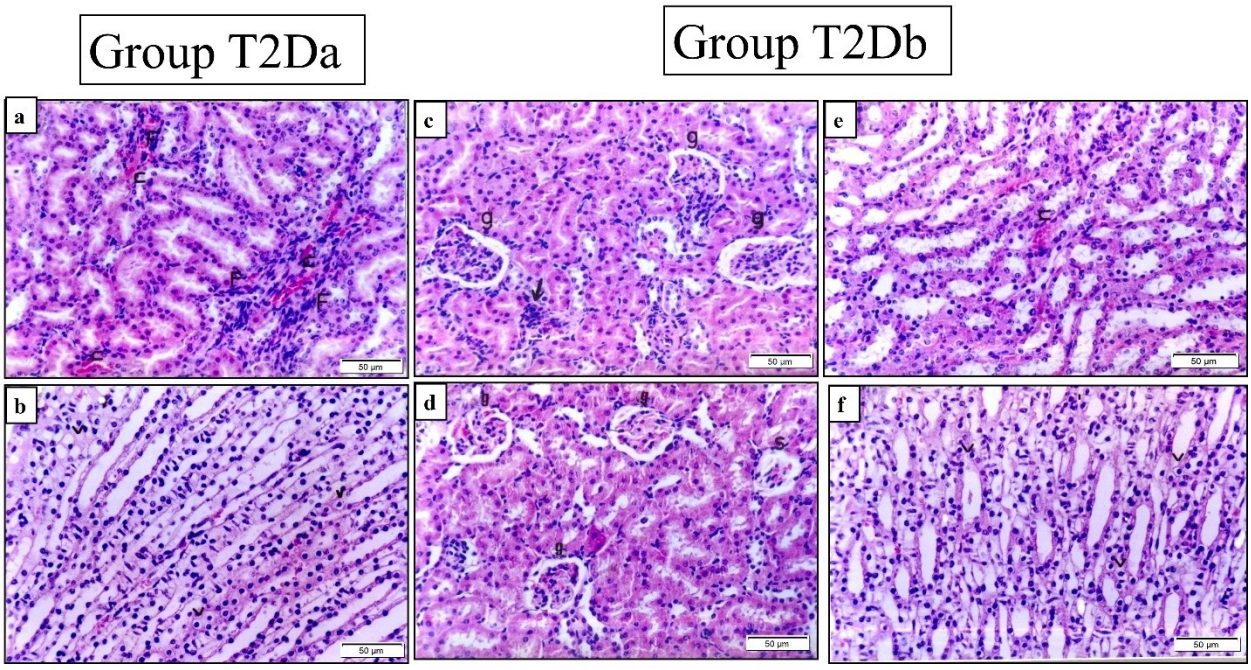

Figure 3A. Multiple fibroblasts (f) detected around congested (c) peritubular capillaries; **B.** Multiple vacuolations (v) detected among the collecting tubules **in subgroup T2Da**. **C.** Minimal cellular infiltrate (arrow) among cortical tubules and normal glomeruli (g); **D.** Multiple normal glomeruli (g) and a shrunken (s) one; **E.** Minimal congestion (c) and **F.** Few vacuolations among apparently normal collecting tubules **in subgroup T2Db**.

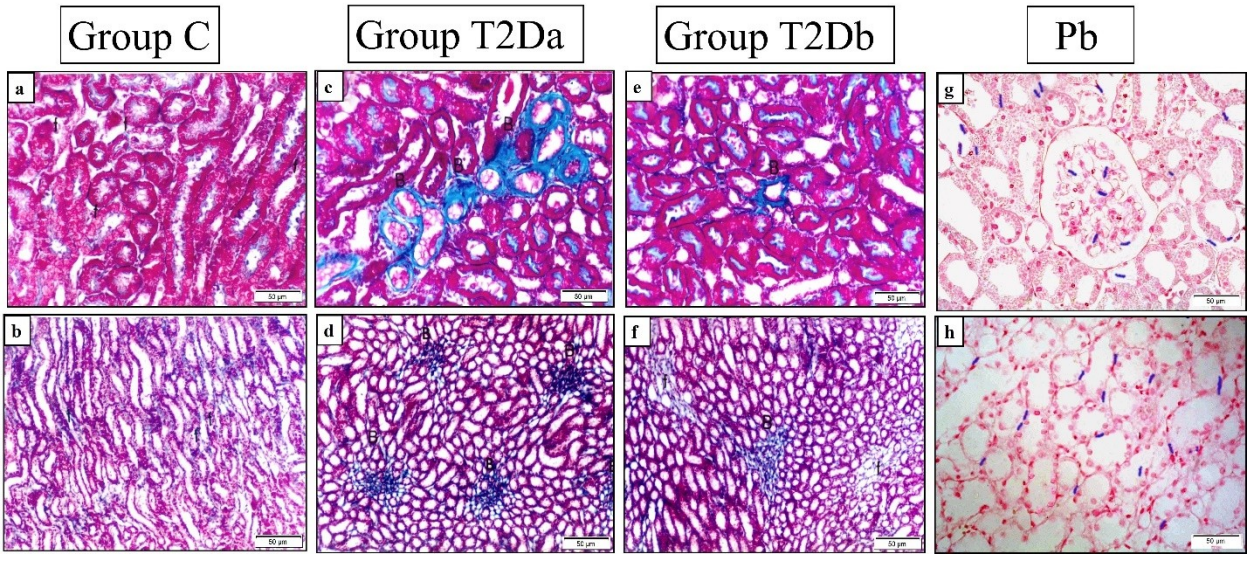

Figure 4. Trichrome stained renal sections, (×200) demonstrated: A. Fine collagen fibers (f) between cortical tubules; **B.** Fine fibers (f) between collecting tubules **in C group; C.** Dense collagen bundles (B) between cortical tubules; **D.** Multiple reticular collagen bundles (B) between collecting tubules **in subgroup T2Da; E.** A dense collagen bundle (B) between cortical tubules; **F.** A reticular collagen bundle (B) and fine fibers (f) between collecting tubules **in subgroup T2Db.** Pb stained sections (×200) showed **G.** Multiple +vely stained spindle cells among the renal glomeruli, cortical tubules and **H.** Collecting tubules.

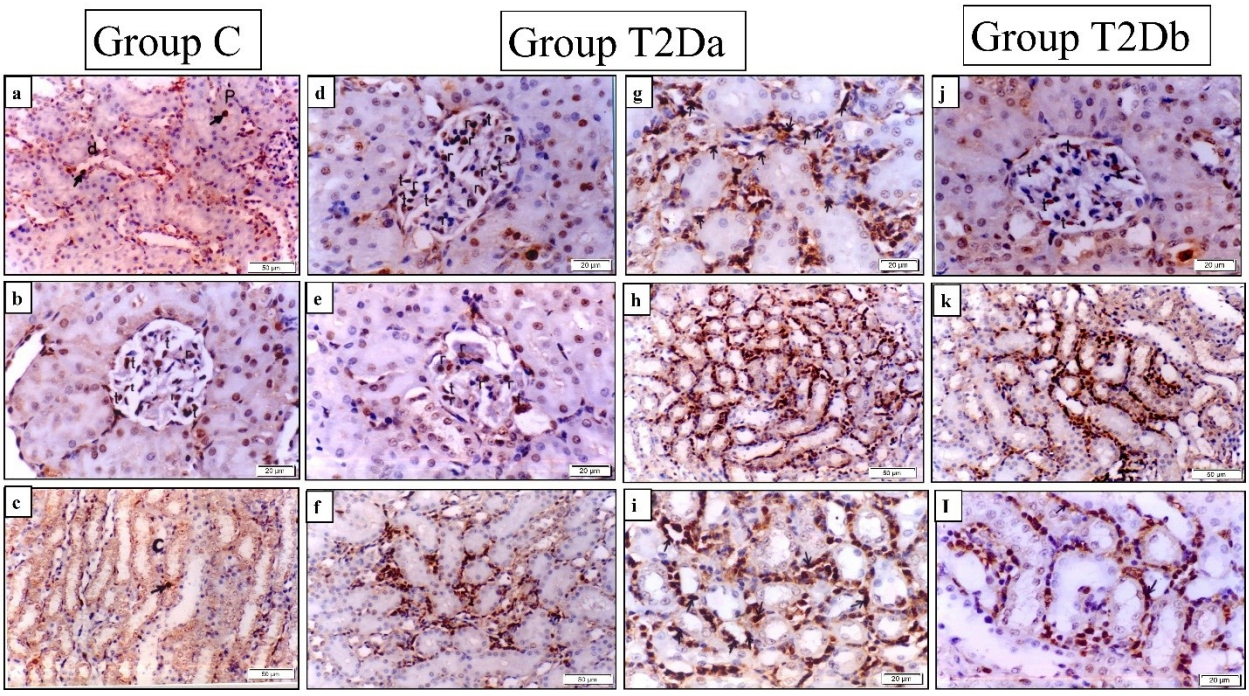

Figure 5. PCNA immunostained sections, clarified; **A.** Few +ve nuclei (N) (arrows) of lining of proximal and distal tubules (×200); **B.** Some +ve flat N (t) and a +ve round (r) nucleus among a glomerulus (×400); **C.** Few +ve N (arrow) of lining of collecting tubules (×200) in **group C;** D. Multiple +ve round (r) and few +ve flat (t) N among a distended glomerulus (×400); **E.** Some +ve round (r) and few +ve flat (t) N among a shrunken glomerulus (×400); **F.** Multiple +ve N among cortical tubules (×200**)**; **G.** Multiple +ve flat interstitial N (arrows) between cortical tubules (×400); **H.** Multiple +ve N among collecting tubules (×200); **I.** Multiple +ve flat interstitial N (arrows) between collecting tubules (×400) in **T2Da subgroup**; **J.** Multiple +ve flat (t) and few +ve round (r) N among a glomerulus (×400); **K.** Some +ve N among tubules at

corticomedullary junction (×200). **L.** Some +ve flat interstitial N (arrows) between the tubules (×400) in **T2Db subgroup**.